Science Advances
AAAS

advances.sciencemag.org/cgi/content/full/4/10/eaas9319/DC1

# Supplementary Materials for

## Transformation of alcohols to esters promoted by hydrogen bonds using oxygen as the oxidant under metal-free conditions

Mingyang Liu, Zhanrong Zhang*, Huizhen Liu, Zhenbing Xie, Qingqing Mei, Buxing Han*

*Corresponding author. Email: hanbx@iccas.ac.cn (B.H.); zhangzhanrong@iccas.ac.cn (Z.Z.)

Published 5 October 2018, *Sci. Adv.* **4**, eaas9319 (2018)
DOI: 10.1126/sciadv.aas9319

**This PDF file includes:**

Fig. S1. The structures of ILs used in this study.
Fig. S2. Product distributions for the oxidative transformation of propanol to propyl propionate in [EMIM] OAc.
Fig. S3. NMR spectra of benzaldehyde and [EMIM] OAc.
Fig. S4. NMR spectra of the mixture of benzaldehyde and [EMIM] OAc.
Fig. S5. $^{1}$H NMR spectra of the reaction media of the oxidative esterification reaction of benzyl alcohol (that is, the reaction in Table 1, entry 1) after 3- (yellow) and 12-hour reaction (green), together with that of the mixture of benzaldehyde and [EMIM] OAc (red).
Fig. S6. Recycling of [EMIM] OAc for oxidative esterification of benzyl alcohol and ethanol.
Fig. S7. Possible acid-base equilibrium in [EMIM] OAc.
Fig. S8. Effects of free carbene (products of the reaction between azolium salts A or B and DBU) on the oxidative reactions of benzyl alcohol and benzyl aldehyde.
Fig. S9. Isotope labeling experiments with $^{18}$O-enriched benzyl alcohol.
Fig. S10. Mass spectra of substrates and products for the experiments with $^{18}$O-enriched benzyl alcohol.
Fig. S11. $^{1}$H NMR spectrum of mixture of benzyl alcohol and [EMIM] OAc (molar ratio of benzyl alcohol to [EMIM] OAc = 1:1).
Fig. S12. $^{1}$H NMR spectrum of mixture of benzyl alcohol and [EMIM] OAc (molar ratio of benzyl alcohol to [EMIM] OAc = 1:5).
Fig. S13. $^{1}$H NMR spectra of mixture of benzyl alcohol and [EMIM] TFA (molar ratio of benzyl alcohol to [EMIM] TFA = 1:1).
Fig. S14. $^{1}$H NMR spectra of mixture of benzyl alcohol and [EMIM] TFA (molar ratio of benzyl alcohol to [EMIM] TFA = 1:5).
Fig. S15. FTIR spectra of benzyl alcohol, [EMIM] OAc, and their mixtures with various molar ratios.
Fig. S16. DOSY NMR spectra.
Fig. S17. $^{1}$H NMR spectrum of [EMIM] OAc before (above) and after (below) drying in vacuum.

Fig. S18. Variation of moisture content and pH of the reaction media during the oxidative esterification reaction.
Fig. S19. Effects of water content for the oxidative esterification of benzyl alcohol.
Table S1. Self-esterification of benzyl alcohol to benzyl benzoate in various ILs with or without additives.
Table S2. Chemical shifts and FWHM of the hydroxyl group resonance band in $^{1}H$ NMR spectra of the mixtures of benzyl alcohol and [EMIM] OAc with various molar ratios.
Table S3. Chemical shifts and FWHM of the hydroxyl group resonance band in $^{1}H$ NMR spectra of mixture of benzyl alcohol and [BMIM] TFA with various molar ratios.
Table S4. Chemical shifts and FWHM of the hydroxyl group resonance band in $^{1}H$ NMR spectra of mixture of benzyl alcohol and [EMIM] $BF_4$ with various molar ratios.
Table S5. Summary of assignments and shifts of frequencies ($cm^{-1}$) of absorption bands in the FTIR spectra in fig. S15. (ν, stretch; s, symmetric; as, antisymmetric).
Table S6. Summary of diffusion coefficients.

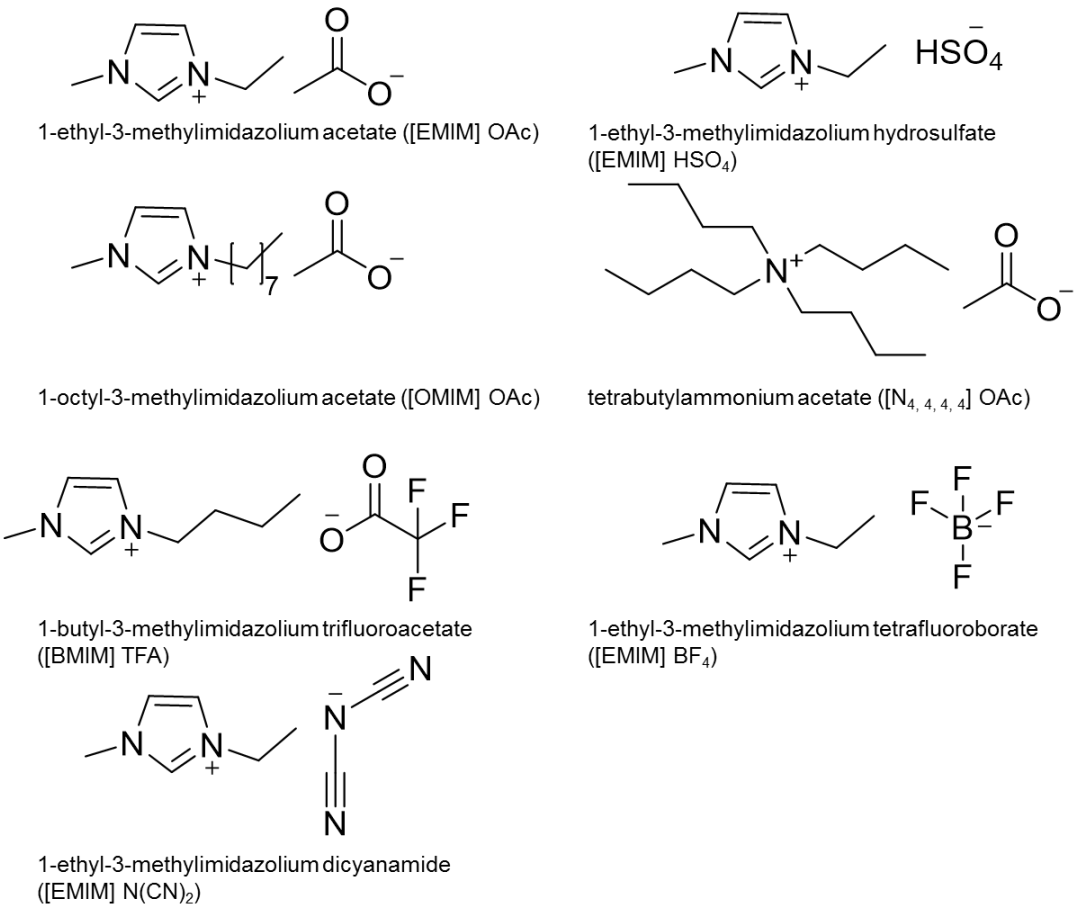


**Fig. S1. The structures of ILs used in this study.**

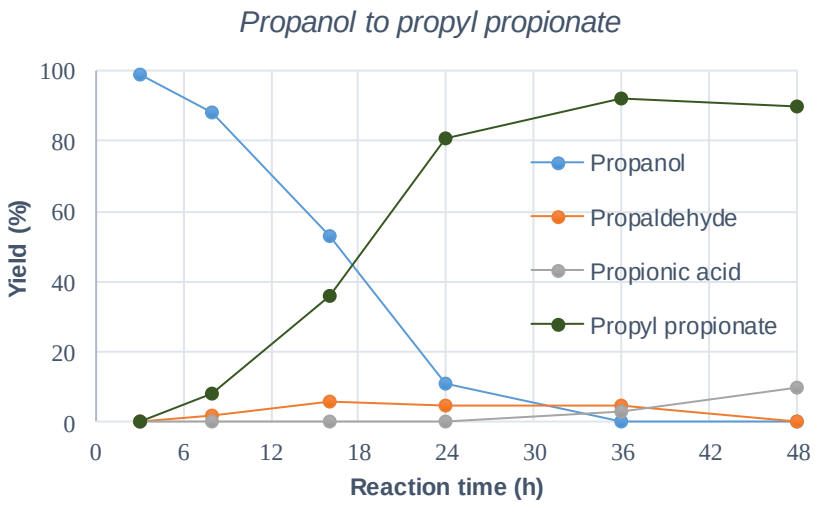


**Fig. S2. Product distributions for the oxidative transformation of propanol to propyl propionate in [EMIM] OAc.** Reaction conditions were the same as those for the reactions in Table 2[c] (2 mmol propanol, 2 MPa $O_2$, 100 $^oC$, 2 g [EMIM] OAc). Yields were determined by GC.

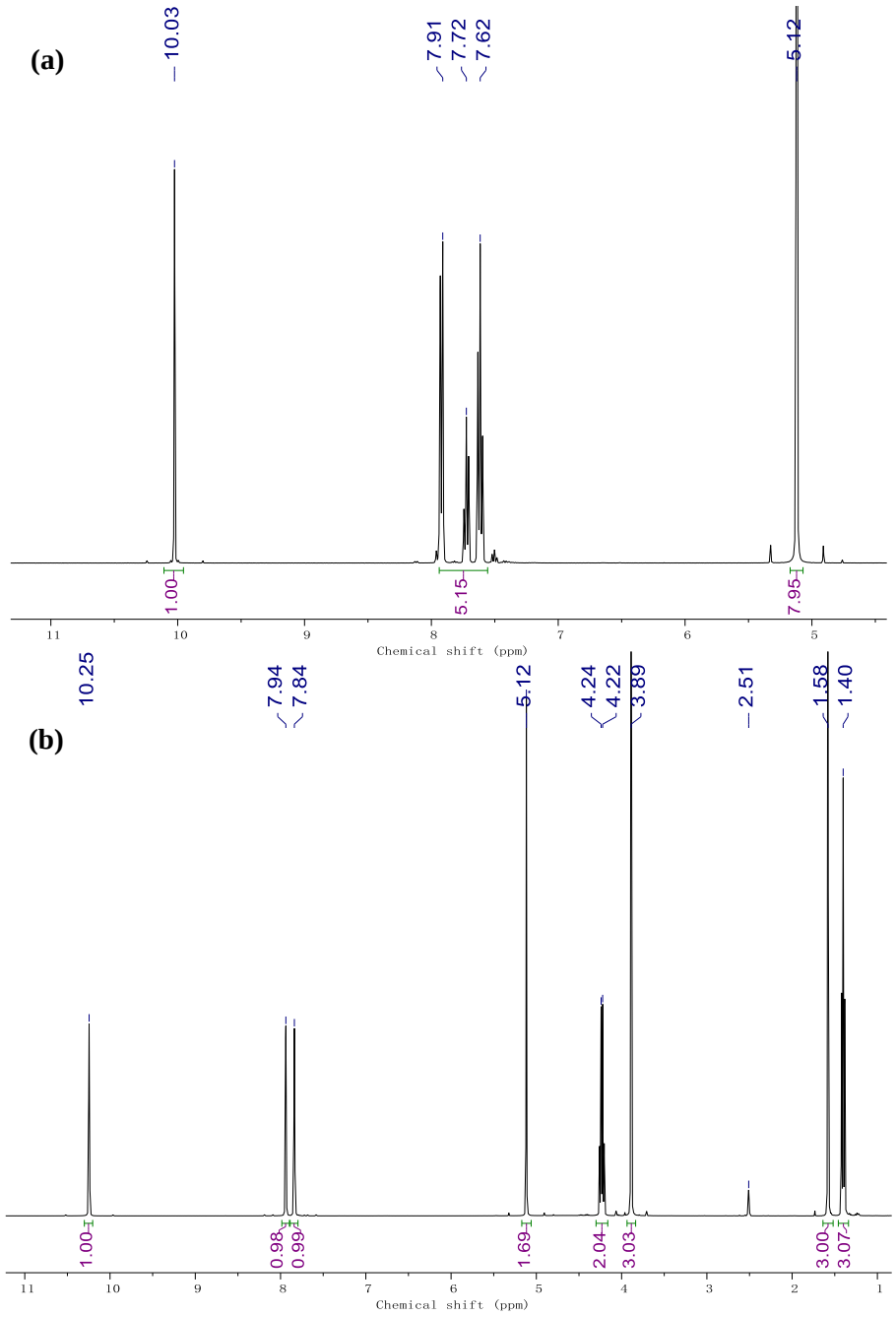


**Fig. S3. NMR spectra of benzaldehyde and [EMIM] OAc.** $^{1}$H NMR spectra of (**a**) benzaldehyde and (**b**) [EMIM] OAc in DMSO-$d_6$. *s*-Trioxane was used as internal standard at 5.12 ppm, spectra were recorded at room temperature.

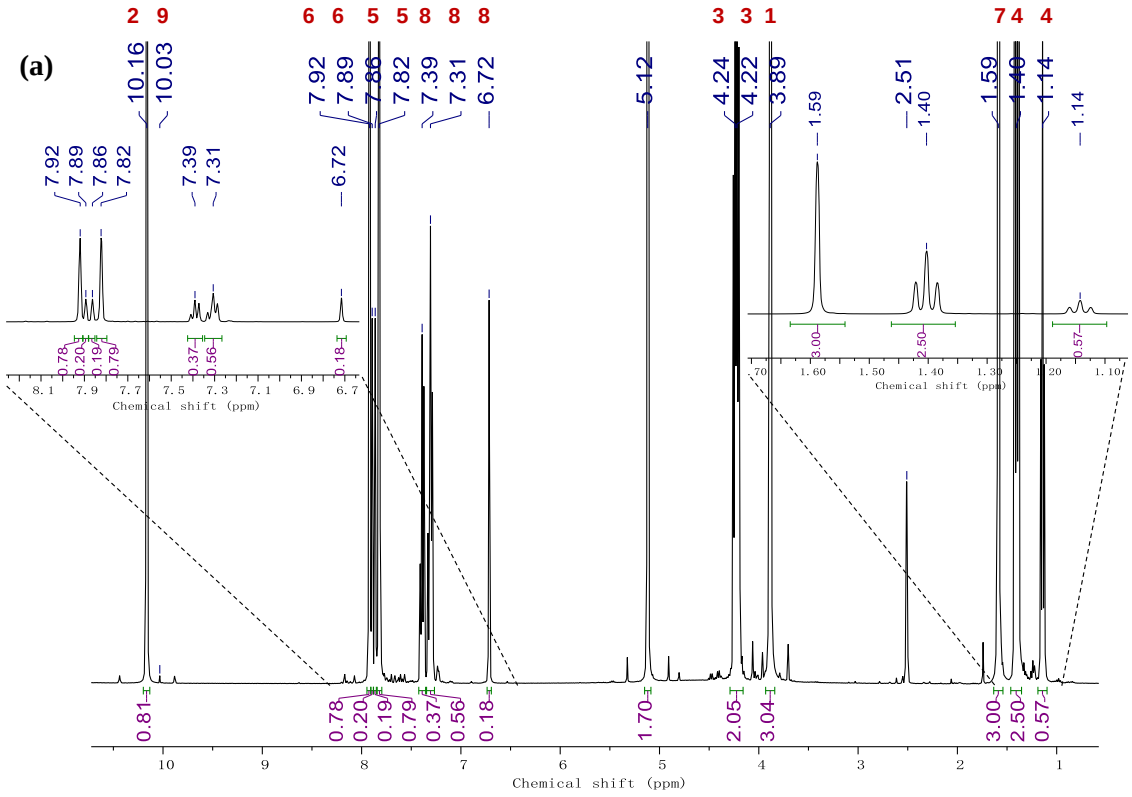


**(b)**

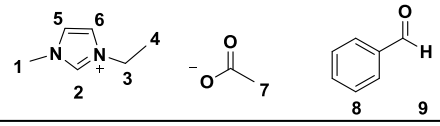

| Different protons | 1 | 2 | 3 | 4 | 5 | 6 | 7 | 8 | 9 |
|---|---|---|---|---|---|---|---|---|---|
| | Chemical shift (ppm) | | | | | | | | |
| Pure IL or aldehyde | 3.89 | 10.25 | 4.24<br>4.22 | 1.40 | 7.84 | 7.94 | 1.58 | 7.91<br>7.72<br>7.62 | 10.03 |
| Mixture of IL and aldehyde | 3.89 | 10.16 | 4.24<br>4.22 | 1.40<br>1.14 | 7.86<br>7.82 | 7.92<br>7.89 | 1.59 | 7.39<br>7.31<br>6.72 | 10.03 |

**Fig. S4. NMR spectra of the mixture of benzaldehyde and [EMIM] OAc.** (**a**) $^{1}$H NMR of the mixture of benzaldehyde (6.2 mg, 0.058 μmol) and [EMIM] OAc (50.0 mg, 0.294 mmol) in DMSO-$d_6$ (0.5 mL). *s*-Trioxane (7.5 mg, 0.083 mmol) was used as internal standard at 5.12 ppm, spectra were recorded at room temperature. (**b**) Summary of H resonance signals of pure benzaldehyde, [EMIM] OAc and their mixture.

By comparing the $^{1}$H NMR spectra of pure benzaldehyde, [EMIM] OAc (fig. S3 a and b) and their mixture (fig. S4 a), it is clear that many proton resonance signals of

benzaldehyde and [EMIM] OAc changed after mixing, which verifies the strong interaction between benzaldehyde and NHC originated from [EMIM] OAc. For instance, the resonance band of aldehyde group centered at 10.03 ppm (9) nearly disappeared in fig. S4 a. The resonance bands of 5-H (5) and 6-H (6) of [EMIM] OAc were split and two new bands were detected at 7.89 and 7.86 ppm. Furthermore, obvious changes of the resonance bands attributed to phenyl group of aldehyde substrate could be observed in the range from 6.7 to 8.0 ppm and a new singlet at 6.72 ppm was detected. Triplet of the 4-H of [EMIM] OAc was split and a new band was detected at 1.14 ppm. By comparing figs. S3 b and S4 a, the integrated band area of the most active proton 2-H (2) decreased from 1.00 to 0.81 after the ionic liquid was mixed with benzaldehyde, due to the interaction between ionic liquid and aldehyde. The high activity of benzaldehyde to NHC renders the characteristic band of aldehyde very weak. However, the abovementioned changes of characteristic resonances bands of either aldehyde or ionic liquid clearly indicates that benzaldehyde was generated and easily consumed even at room temperature.

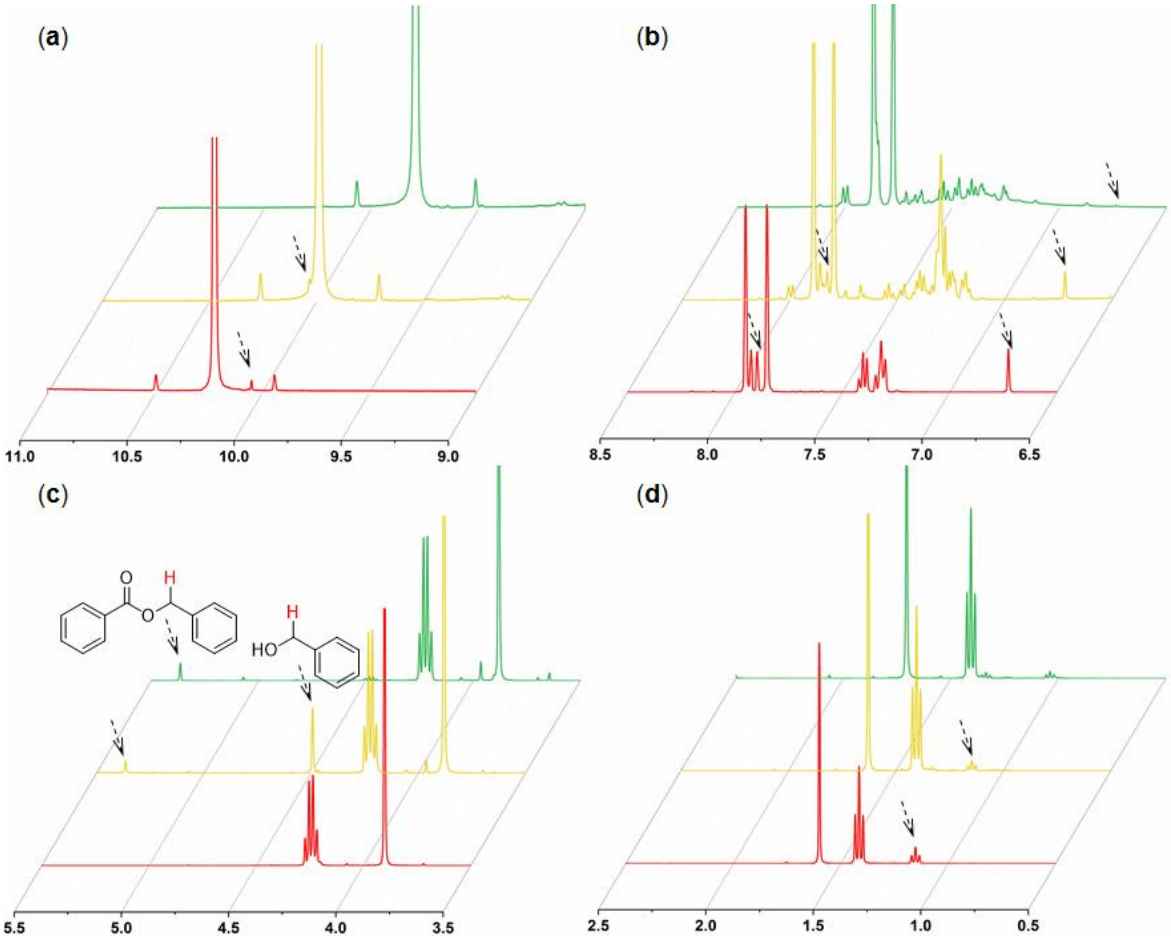


**Fig. S5. $^{1}$H NMR spectra of the reaction media of the oxidative esterification reaction of benzyl alcohol (that is, the reaction in Table 1, entry 1) after 3- (yellow) and 12-hour reaction (green), together with that of the mixture of benzaldehyde and [EMIM] OAc (red).** The spectra were recorded at room temperature in DMSO-$d_6$. For convenience, we divided the spectra into four parts: (**a**) 11.0-9.0 ppm. (**b**) 8.5-6.5 ppm. (**c**) 5.5-3.5 ppm. (**d**) 2.5-0.5 ppm. Characteristic resonance bands are highlighted by arrows.

Figure S5 illustrates the $^{1}$H NMR spectra of reaction media originated from the oxidative esterification of benzyl alcohol recorded after 3 h (yellow) and 12 h reaction (green). In comparison with the spectra of the mixture of benzaldehyde and [EMIM] OAc (red), characteristic resonance bands of benzyl alcohol (4.49 ppm) and benzyl benzoate (5.36 ppm) were detected (fig. S5 c). Notably, characteristic resonance bands originated from the interaction of benzaldehyde and [EMIM] OAc (as shown and discussed in fig. S4) were also detected at 10.03, 7.89, 7.86, 6.72 and 1.14 ppm. From the spectrum recorded

after 12 h reaction, characteristic resonance bands of benzyl alcohol and benzaldehyde nearly disappeared, while that of benzyl benzoate (5.36 ppm) was detected. These results clearly indicate that aldehyde represents a highly active intermediate during the oxidative esterification reactions, which supports and is in good consistency with our proposed mechanism.

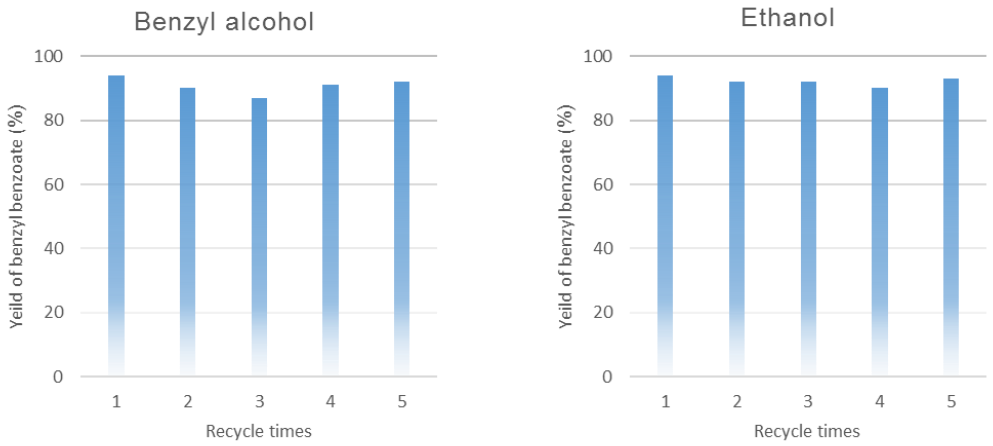


**Fig. S6. Recycling of [EMIM] OAc for oxidative esterification of benzyl alcohol and ethanol.** Reaction conditions were the same as those for the reaction in Table 1 (2 mmol benzyl alcohol, 1 MPa $O_2$, 2 g IL, 12 h, 80 °C) and Table 2 (2 mmol ethanol, 2 MPa $O_2$, 2 g ILs, 36 h, 100 °C). Yields were determined by GC.

**Table S1. Self-esterification of benzyl alcohol to benzyl benzoate in various ILs with or without additives.**

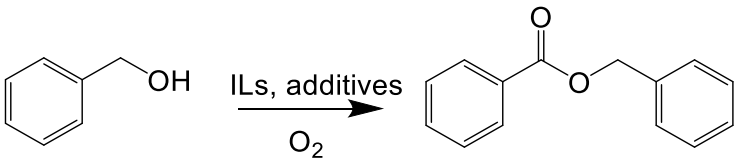


| Entry | ILs | Additives | Time (h) | Conversion (%) | Yield (%) |
|---|---|---|---|---|---|
| 1 | [EMIM] OAc | | 3 | 38 | 20 |
| 2 | [EMIM] OAc | | 8 | 90 | 73 |
| 3 | [EMIM] OAc | | 12 | >99 | 94 |
| 4 | [EMIM] OAc | | 16 | >99 | 90 |
| 5[b] | [EMIM] OAc | DBU | 3 | 43 | 26 |
| 6[b] | [EMIM] OAc | DBU | 8 | >99 | 85 |
| 7[b] | [EMIM] OAc | DBU | 12 | >99 | 90 |
| 8[b] | [EMIM] OAc | DBU | 16 | >99 | 91 |
| 9[c] | [EMIM] OAc | TEMPO | 12 | >99 | 95 |
| 10[c] | [EMIM] OAc | BHT | 12 | >99 | 92 |
| 11 | [BMIM] OAc | | 12 | >99 | 0 |
| 12 | [OMIM] OAc | | 12 | <1 | 0 |
| 13[d] | [EMIM] OAc | | 3 | >99 | >99 |
| 14[e] | [EMIM] OAc | | 12 | 3 | <1 |
| 15[f] | [EMIM] OAc | | 12 | 9 | 0 |
| 16[g] | [EMIM] OAc | | 12 | <1 | 0 |
| 17[h] | [EMIM] OAc | | 36 | >99 | 88 |
| 18[i] | [EMIM] OAc | | 12 | >99 | 47 |

[a]Reaction condition: 2 mmol benzyl alcohol, 2 g ILs, 1 MPa $O_2$, 80 °C. [b]2 mmol DBU was added. [c]0.2 mmol TEMPO or BHT was added. [d]2 mmol benzaldehyde was added. [e]2 MPa $N_2$ was used instead of $O_2$. [f]Benzyl aldehyde was used as substrate. [g]Benzoic acid was used as substrate. [h]200 mmol (21.6 g) benzyl alcohol, 100 g ILs, 1 MPa $O_2$, 80 °C, 36 h. [i]1 mmol benzyl alcohol, 0.5 mmol 4-metylbenzyl alcohol, 2 g ILs, 1 MPa $O_2$, 80 °C. Cross-esterification products including 4-methylbenzyl 4-methylbenzoate (9%), 4-methylbenzyl benzoate (17%) and benzyl 4-methylbenzoate (18%) were also detected. Yields were based on the total 1.5 mmol alcohol.

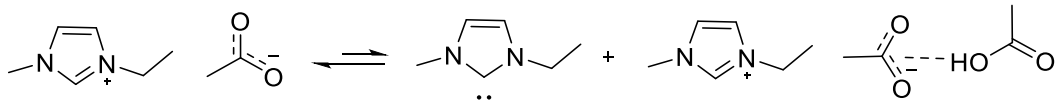

**Fig. S7. Possible acid-base equilibrium in [EMIM] OAc.**

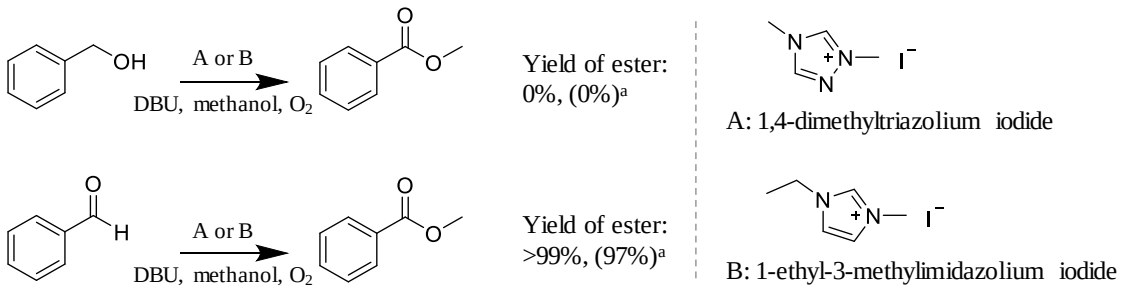


**Fig. S8. Effects of free carbene (products of the reaction between azolium salts A or B and DBU) on the oxidative reactions of benzyl alcohol and benzyl aldehyde.** Reaction conditions: 0.5 mmol substrate, 2 mL methanol, 20 mol % of azolium salts, 1.2 equiv of DBU, 1 MPa $O_2$, 80 °C, 12 h. Yields were determined by GC using *n*-dodecane as internal standard. [a]Azolium salt B was used, 60 mol % of azolium salts.

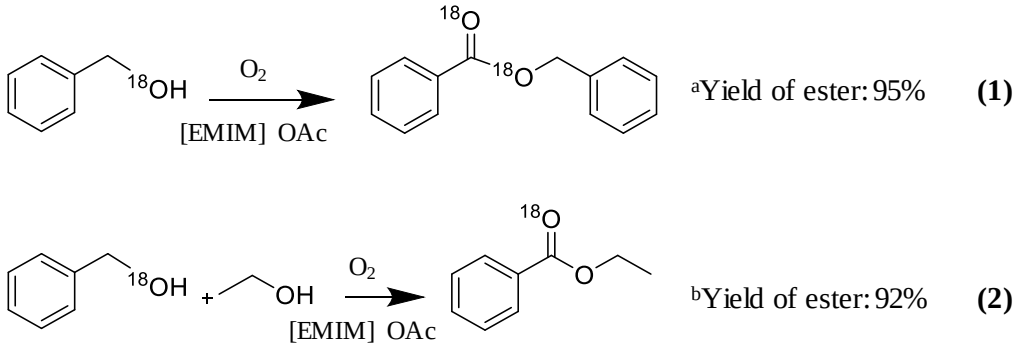


**Fig. S9. Isotope labeling experiments with $^{18}O$-enriched benzyl alcohol.** Reaction conditions: [a]2 mmol benzyl alcohol, 1 MPa $^{16}O_2$, 2 g ILs, 12 h, 80 °C. [b]2 mmol benzyl alcohol, 8 mmol ethanol, 2 MPa $^{16}O_2$, 2 g [EMIM] OAc, 12 h, 80 °C. Detailed mass spectra of these molecules with oxygen isotope are presented in fig. S10.

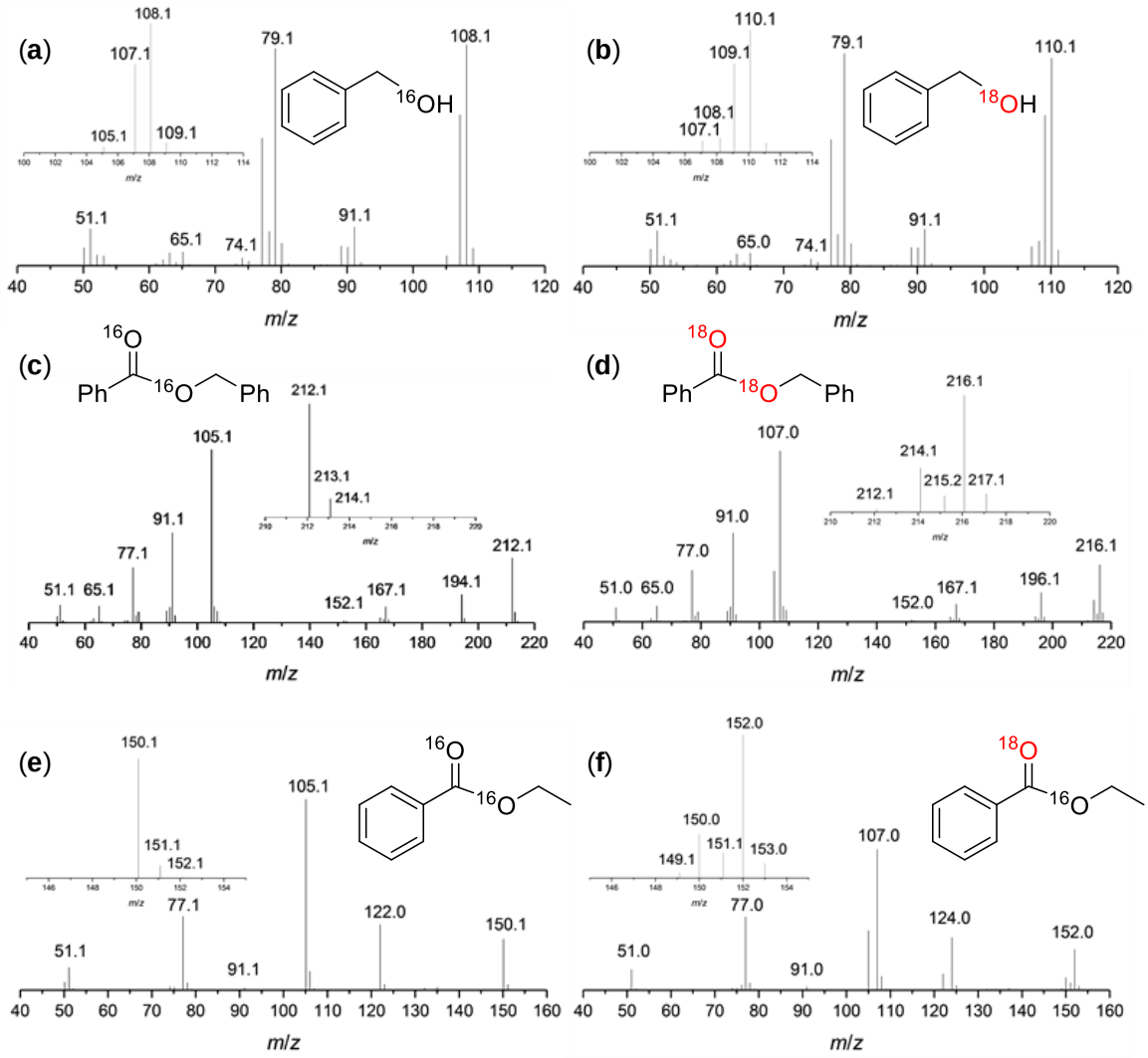


**Fig. S10. Mass spectra of substrates and products for the experiments with $^{18}$O-enriched benzyl alcohol.** (**a**) Benzyl alcohol; (**b**) $^{18}$O-enriched benzyl alcohol (height ratio of peak at *m*/*z* 110.1:108.1 = 6.7:1); (**c**) Benzyl benzoate; (**d**) $^{18}$O-enriched benzyl benzoate in equation 1 of fig. S9 (height ratio of peak at *m*/*z* 216.1:214.1:212.1 = 39.8:14.1:1). (**e**) Ethyl benzoate; (**f**) Half $^{18}$O-enriched ethyl benzoate in equation 2 of fig. S9 (height ratio of peak at *m*/*z* 152.0:150.0 = 3.7:1).

For the oxidative self-esterification of $^{18}$O-enriched benzyl alcohol in [EMIM] OAc and $^{16}O_2$, similar yield of ester product was obtained and the two O atoms in benzyl benzoate were assigned to $^{18}$O. For the cross-esterification between $^{18}$O-enriched benzyl alcohol and ethanol, the O atom of the carbonyl group of generated ethyl benzoate was assigned to $^{18}$O. Hence, these results clearly indicate that no oxygen atom obviously transferred from

$O_2$ to alcohol substrate or intermediates and no isotope exchange occurred between the substrate, intermediates and products during the reaction.

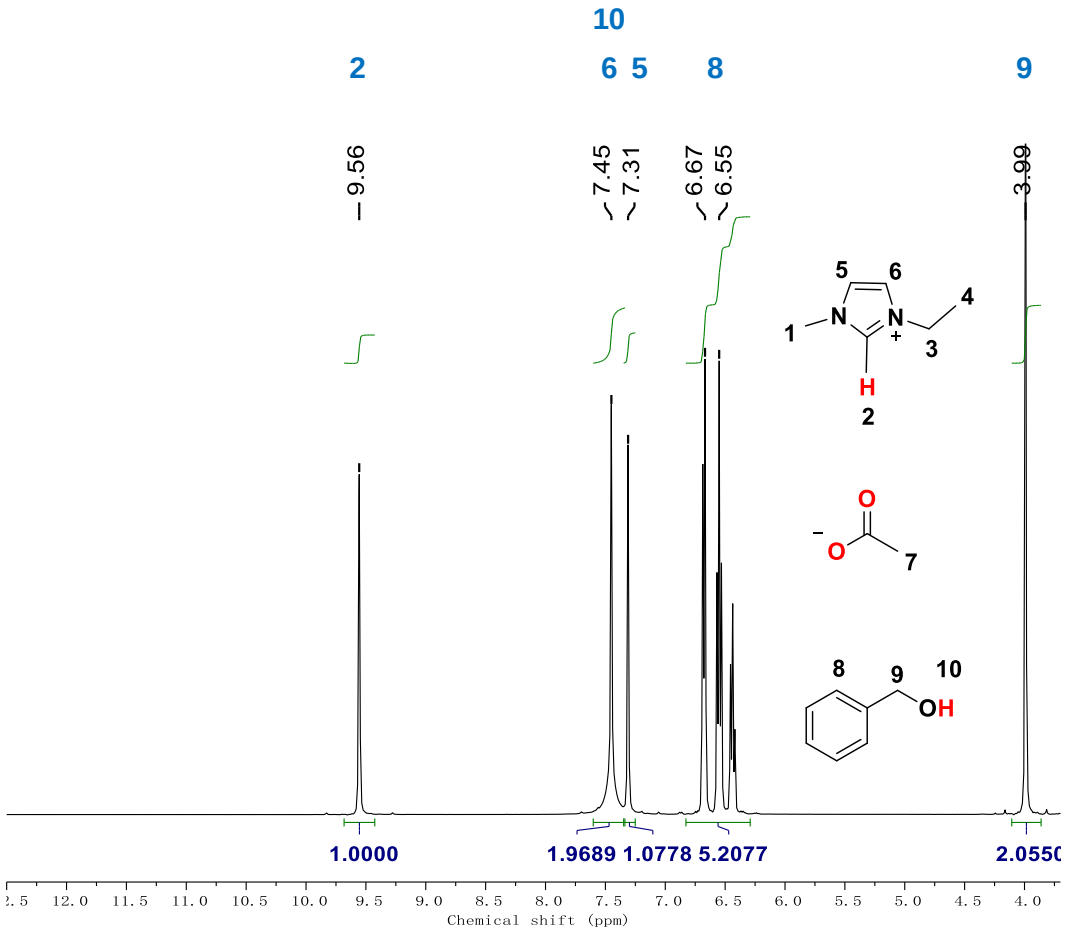


**Fig. S11. $^1$H NMR spectrum of mixture of benzyl alcohol and [EMIM] OAc (molar ratio of benzyl alcohol to [EMIM] OAc = 1:1).** The integrals were based on the 2-protons of [EMIM] cation. The resonance band of hydroxyl protons at 7.45 ppm was overlapped by that of the 6-protons of [EMIM] cation.

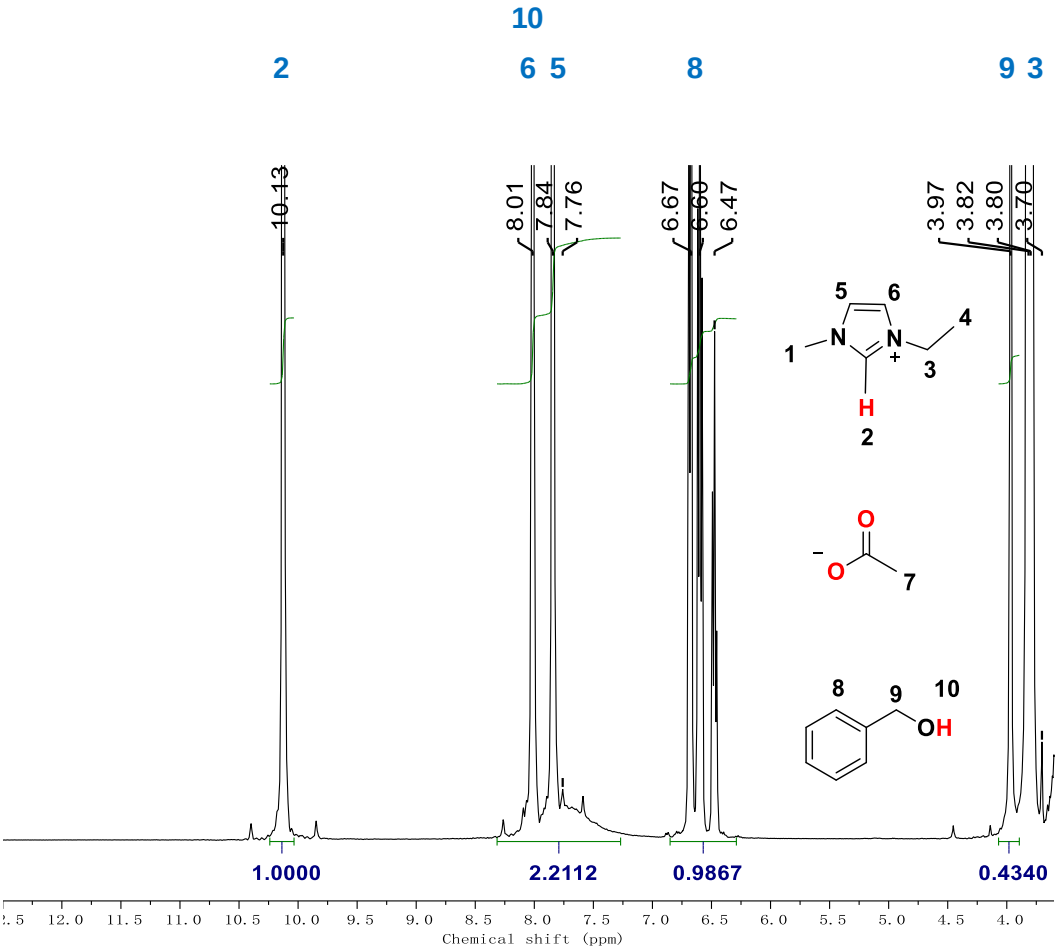


**Fig. S12. $^{1}$H NMR spectrum of mixture of benzyl alcohol and [EMIM] OAc (molar ratio of benzyl alcohol to [EMIM] OAc = 1:5).** The integrals were based on the 2-protons of [EMIM] cation. The resonance band of hydroxyl protons at 7.76 ppm was covered by that of the 5-protons of [EMIM] cation.

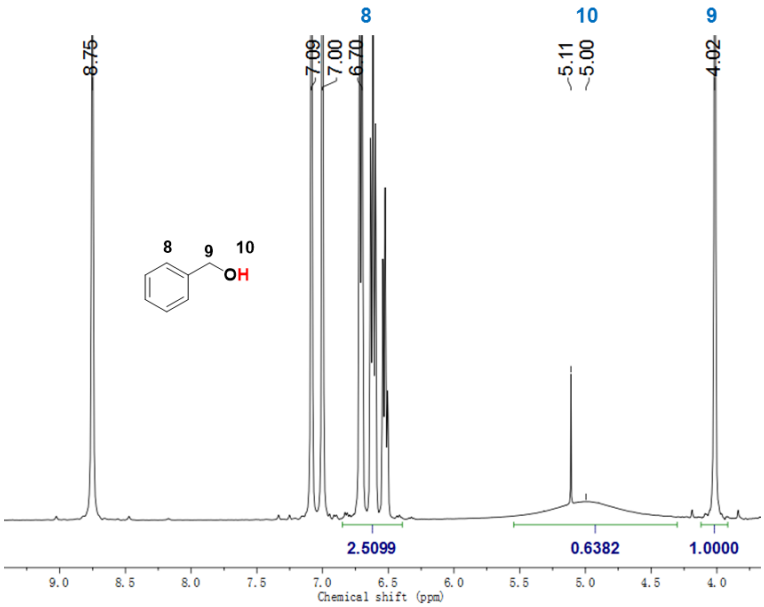


**Fig. S13. $^{1}$H NMR spectra of mixture of benzyl alcohol and [EMIM] TFA (molar ratio of benzyl alcohol to [EMIM] TFA = 1:1).** The integrals were based on the β-protons of benzyl alcohol. The resonance band of hydroxyl protons locates at 5.00 ppm (band 10).

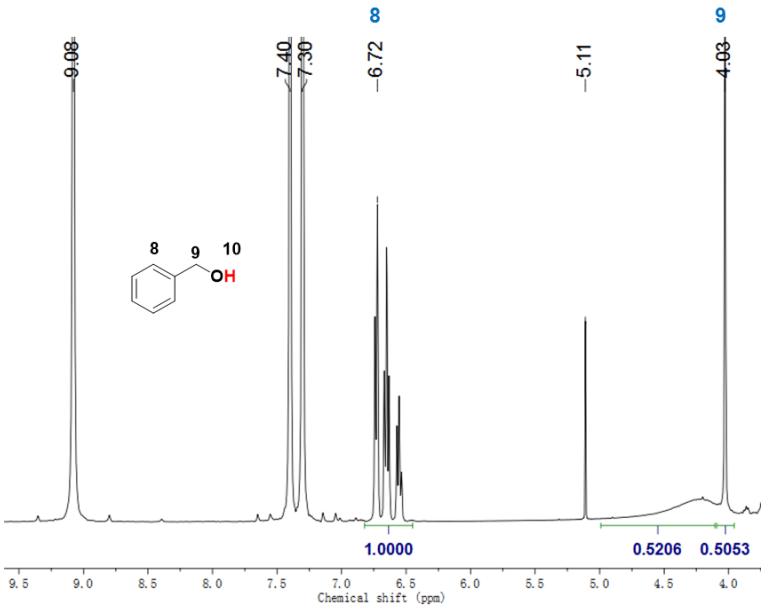


**Fig. S14. $^{1}$H NMR spectra of mixture of benzyl alcohol and [EMIM] TFA (molar ratio of benzyl alcohol to [EMIM] TFA = 1:5).**

**Table S2. Chemical shifts and FWHM of the hydroxyl group resonance band in $^{1}H$ NMR spectra of the mixtures of benzyl alcohol and [EMIM] OAc with various molar ratios.**

| Molar Ratios of Benzyl alcohol to [EMIM] OAc | Chemical shift (ppm) | FWHM (ppm) |
|---|---|---|
| 1 : 0 | 4.63 | 0.02 |
| 10 : 1 | 5.57 | 0.02 |
| 5 : 1 | 6.16 | 0.04 |
| 1 : 1 | 7.45 | 0.11 |
| 1 : 5 | 7.76 | 0.65 |

With the increasing of [EMIM] OAc content in the mixture, the resonance band attributed to hydroxyl group of benzyl alcohol shifts toward the downfield region from 4.63 ppm to 7.76 ppm. This effect is primarily due to the formation of hydrogen bond between hydroxyl protons and the acetate anions. Meanwhile, the FWHM values of the resonance band increased from 0.02 to 0.65, indicating the interaction/coordination between hydroxyl groups and the 2-H of imidazole ring.

**Table S3. Chemical shifts and FWHM of the hydroxyl group resonance band in $^{1}H$ NMR spectra of mixture of benzyl alcohol and [BMIM] TFA with various molar ratios.**

| Molar Ratios of Benzyl alcohol to [BMIM] TFA | Chemical shift (ppm) | FWHM (ppm) |
|---|---|---|
| 1 : 0 | 4.63 | 0.02 |
| 10 : 1 | 4.94 | 0.31 |
| 5 : 1 | 5.06 | 0.36 |
| 1 : 1 | 5.00 | 0.95 |
| 1 : 5 | | |

In [BMIM] TFA, the methyl protons in acetate were replaced by electrophilic fluorine atoms. Thus, the density of electron cloud of the anion is more equalized, and the ability to form hydrogen bonds with hydroxyl groups becomes much weaker. The shift of resonance

band of hydroxyl group of benzyl alcohol was very small (less than 0.5 ppm) upon addition of same amount of [BMIM] TFA in comparison to those in [EMIM] OAc. (Fig. 2, table S3). The FWHM values of this resonance band increased slightly, indicating the interaction/coordination between hydroxyl groups and the 2-H of imidazole ring.

**Table S4. Chemical shifts and FWHM of the hydroxyl group resonance band in $^{1}H$ NMR spectra of mixture of benzyl alcohol and [EMIM] $BF_4$ with various molar ratios.**

| Molar Ratios of Benzyl alcohol to [EMIM] $BF_4$ | Chemical shift (ppm) | FWHM (ppm) |
|---|---|---|
| 1 : 0 | 4.63 | 0.02 |
| 10 : 1 | 4.35 | 0.14 |
| 5 : 1 | 4.09 | 0.18 |
| 1 : 1 | 3.47 | 0.20 |
| 1 : 5 | 3.02 | 0.20 |

In contrast to [EMIM] OAc and [BMIM] TFA, the characteristic resonance band attributed to hydroxyl group of benzyl alcohol shifts towards the up-field region from 4.63 to 3.02 with the increasing of [EMIM] $BF_4$ content in the mixture. The FWHM values of the resonance band also increased, indicating the interaction/coordination between hydroxyl groups and the 2-H of imidazole ring.

Unlike acetate or $TFA^-$, $BF_4^-$ anion cannot form hydrogen bonds with alcohol substrates. For the mixtures containing benzyl alcohol and [EMIM] $BF_4$, the characteristic hydroxyl resonance band of hydroxyl groups in benzyl alcohol shifts toward the up-field region, as benzyl alcohol is in shielding cone of the aromatic imidazolium ring of [EMIM] $BF_4$ (Fig. 2, table S4).

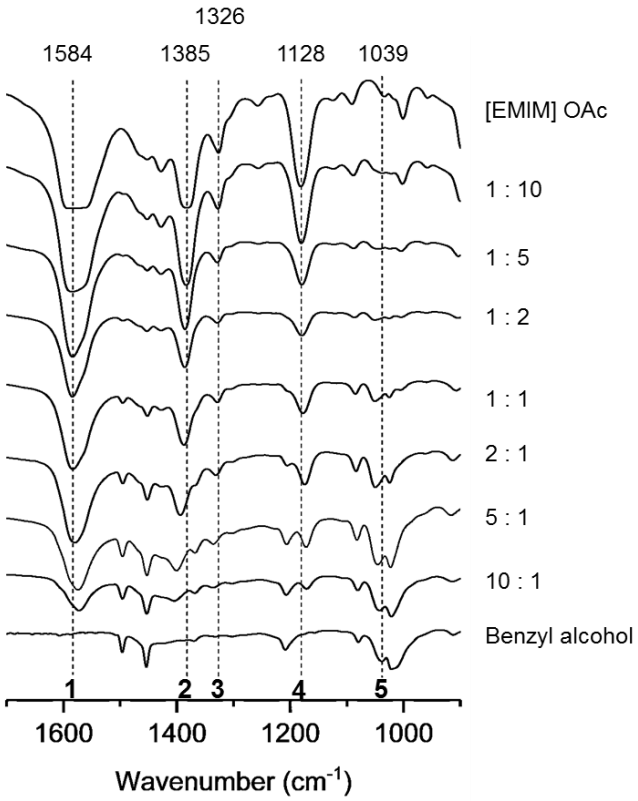


**Fig. S15. FTIR spectra of benzyl alcohol, [EMIM] OAc, and their mixtures with various molar ratios.** The molar ratios shown in the figure are benzyl alcohol to [EMIM] OAc. Assignment of absorption bands and analysis are shown table S5.

**Table S5. Summary of assignments and shifts of frequencies ($cm^{-1}$) of absorption bands in the FTIR spectra in fig. S15. (v, stretch; s, symmetric; as, antisymmetric).**

| No. | Species | Frequency ($cm^{-1}$) | Assignments |
|---|---|---|---|
| 1 | [EMIM] OAc | 1584-1571 | $\nu_{as}$(COO) |
| 2 | [EMIM] OAc | 1385-1404 | $\nu$(N-$CH_2$) |
| 3 | [EMIM] OAc | 1326-1336 | $\nu_s$(COO) |
| 4 | [EMIM] OAc | 1182-1169 | $\nu$(N-$CH_3$) |
| 5 | Benzyl alcohol | 1039-1051 | $\nu$(C-O) |

From the FT-IR spectrum of benzyl alcohol, characteristic absorption band for the C-O stretching vibration of hydroxyl group of benzyl alcohol is observed at 1039 $cm^{-1}$. With

increasing of [EMIM] OAc content in the mixture, the absorption band shifts to around 1051 $cm^{-1}$. Similar shifts of absorption bands for either imidazolium cation (labeled as 2, 4 in fig. S15) and acetate anion (labeled as 1, 3 in fig. S15) could also be clearly observed. The shifts of characteristic infrared absorption bands indicate the interaction between the imidazolium cation, acetate anion and alcohol substrate.

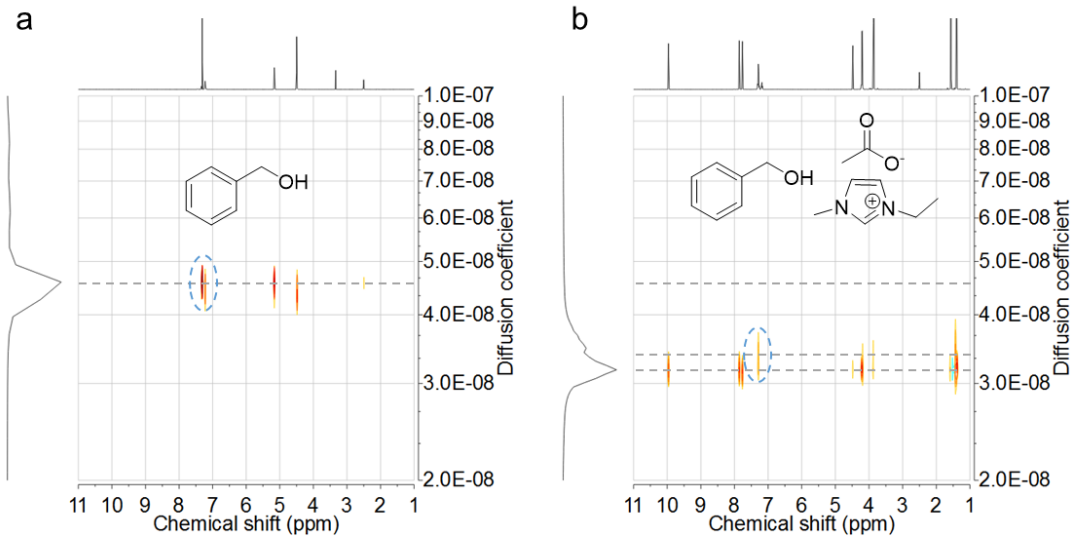


**Fig. S16**. **DOSY NMR spectra.** $^{1}$H-DOSY NMR spectra of (**a**) benzyl alcohol and (**b**) the mixture of benzyl alcohol and [EMIM] OAc. The signals of phenyl proton are highlighted by blue circles. Details of diffusion coefficient are summarized in table S6.

$^{1}$H-DOSY NMR characterization of benzyl alcohol and its mixture with [EMIM] OAc was conducted (fig. S16). Table S6 summarizes the diffusion coefficients of the phenyl and benzyl protons of benzyl alcohol. The diffusion coefficient of both phenyl proton and benzyl proton of benzyl alcohol decreased when benzyl alcohol was mixed with [EMIM] OAc. The decrease in diffusion coefficient results from and reflects the interaction between [EMIM] OAc and benzyl alcohol.

**Table S6**. **Summary of diffusion coefficients.** Diffusion coefficients of phenyl and benzyl protons of benzyl alcohol in the $^{1}$H-DOSY NMR spectra of (**a**) benzyl alcohol and (**b**) the mixture of benzyl alcohol and [EMIM] OAc.

| | Benzyl alcohol | | Benzyl alcohol + EMIM Ac | |
|---|---|---|---|---|
| | Chemical shift | Diffusion coefficient/$m^2 \cdot s^{-1}$ | Chemical shift | Diffusion coefficient/$m^2 \cdot s^{-1}$ |
| Phenyl proton | 7.387-7.265 | 4.431E-10 | 7.392-7.229 | 3.594E-10 |
| | 7.265-7.143 | 4.406E-10 | 7.229-7.080 | 3.497E-10 |
| Benzyl proton | 4.566-4.411 | 4.510E-10 | 4.593-4.403 | 3.924E-10 |

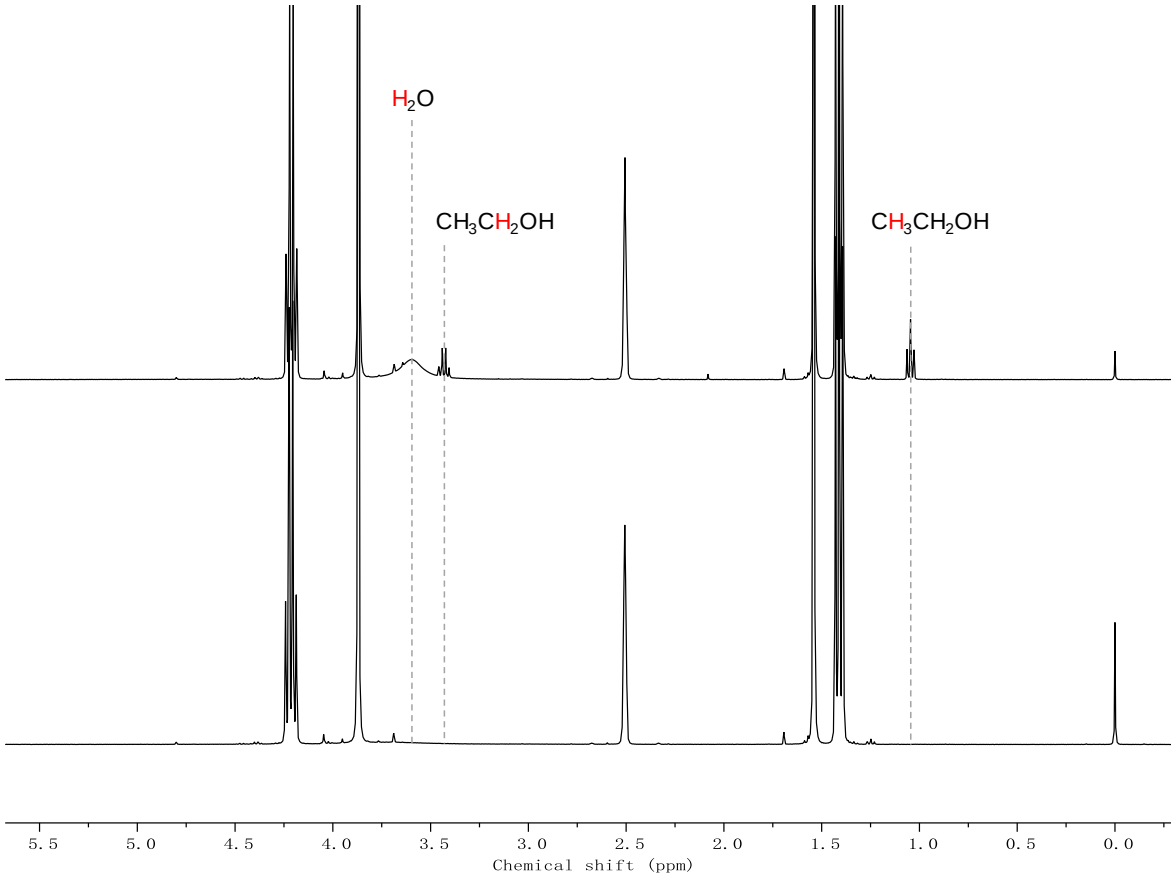


**Fig. S17. $^{1}$H NMR spectrum of [EMIM] OAc before (above) and after (below) drying in vacuum.**

Due to the hygroscopic nature of ILs, trace amounts of water and organic impurities such as ethanol unavoidably present in the commercial supplied ILs. Hence, before use, they were dried under in vacuo at 80 $^{o}$C for 24 h to remove these impurities which otherwise might interfere with the catalytic reactions. From fig. S17, it is obvious that the resonance bands of water and ethanol were disappeared after drying, indicating that they were completely removed after drying.

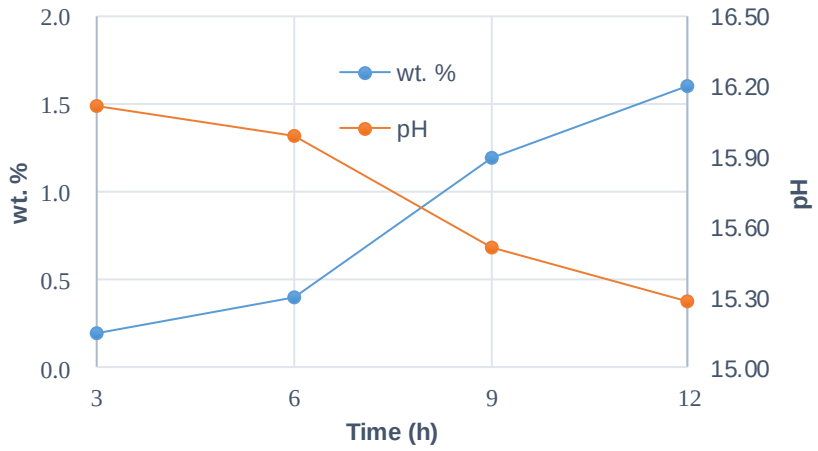


**Fig. S18. Variation of moisture content and pH of the reaction media during the oxidative esterification reaction.** The reaction conditions are the same as those of entry 1 in Table 1. The reaction time is from 3 h to 12 h. During the reaction, the moisture content is slightly increased and the pH of reaction media slightly decreased.

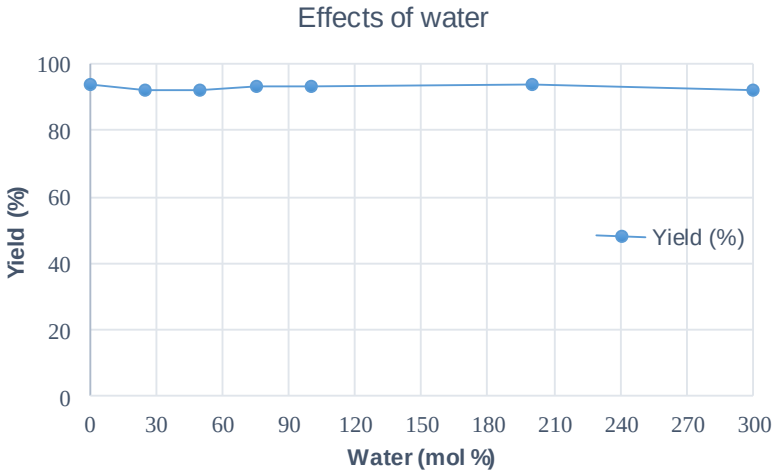


**Fig. S19. Effects of water content for the oxidative esterification of benzyl alcohol.** The reaction conditions are the same as those of entry 1 in Table 1, except additional water was added.